14. B. C. Larson, C. W. White, T. S. Noggle, J. F. Barhorst, D. M. Mills, *Appl. Phys. Lett.* **42**, 282 (1983).
15. M. Caffrey, *Biochemistry* **24**, 4826 (1985).
16. J. K. Blasie *et al.*, *Biophys. J.* **48**, 9 (1985).
17. J. A. McCray, L. Herbette, T. Kihara, D. R. Trentham, *Proc. Natl. Acad. Sci. U.S.A.* 77, 7237 (1980).
18. Time-resolved muscle diffraction studies are reviewed by H. E. Huxley and A. R. Faruqi, *Annu. Rev. Biophys. Bioeng.* **12**, 381 (1983).
19. J. S. Davis and H. Gutfreund, *FEBS Lett.* **72**, 199 (1976).
20. See, for instance, A. J. C. Wilson, *Elements of X-ray Crystallography* (Addison-Wesley, Reading, MA, 1970).
21. K. Moffat, D. Szebenyi, D. Bilderback, *Science* **223**, 1423 (1984); K. Moffat, D. Bilderback, W. Schildkamp, K. Volz, *Nucl. Instrum. Methods* **A246**, 627 (1986).
22. J. Hadju *et al.*, *EMBO J.* **6**, 539 (1987).
23. K. Moffat, D. Bilderback, W. Schildkamp, D. Szebenyi, R. Loane, in *Structural Biological Applications of X-ray Absorption, Scattering and Diffraction*, B. Chance and H. Bartunik, Eds. (Academic Press, New York, 1986); J. R. Helliwell, *J. Mol. Struct.* **130**, 63 (1985).
24. M. Harding, S. Maginn, P. Machin, J. Campbell, I. Clifton, *Daresbury Lab. Inf. Q. Protein Cryst.* **19**, 43 (1986).
25. S. M. Gruner, J. R. Milch, G. T. Reynolds, *Nucl. Instrum. Methods* **195**, 67 (1982).
26. U. W. Arndt, *J. Appl. Crystallogr.* **19**, 145 (1986).
27. D. W. Smits and E. H. Wiegenga, *Acta Crystallogr.* **9**, 520 (1956); H. Moriomoto and R. Uyeda, *ibid.* **16**, 1107 (1963).
28. The dynamic range may be defined in many ways. For the purposes of this article it is defined as the ratio of the saturated signal to the root-mean-square noise per resolution element, or pixel, per frame readout. See S. M. Gruner, J. R. Milch, G. T. Reynolds, *IEEE Trans. Nucl. Sci.* **NS-25**, 562 (1978); S. M. Gruner and J. R. Milch, *Trans. Am. Crystallogr. Assoc.* **18**, 149 (1982).
29. J. Miyahara, K. Takahashi, Y. Amemiya, N. Kamiya, Y. Satow, *Nucl. Instr. Methods* **A246**, 572 (1986); Y. Amemiya, K. Wakabayashi, H. Tanaka, Y. Ueno, J. Miyahara, *Science* **237**, 164 (1987); K. Moffat *et al.*, *Nucl. Instrum. Methods*, in press; B. R. Whiting, J. F. Owen, B. H. Rubin, *ibid.*, in press.
30. P. Crane and M. Davis, *Publ. Astron. Soc. Pac.* **87**, 207 (1975).
31. J. A. Hall, in *Applied Optics and Optical Engineering*, R. R. Shannon and J. C. Wyant, Eds. (Academic Press, New York, 1980), vol. 8.
32. See, for example, J.-P. Baluteau and S. D'Odurico, Eds., *The Optimization of the Use of CCD Detectors in Astronomy*, conference and workshop proceedings, No. 25 (European Southern Observatory, Munich, 1986).
33. J. H. Chappell and S. S. Murray, *Nucl. Instrum. Methods* **221**, 159 (1984).
34. H. W. Deckman and S. M. Gruner, *ibid.* **A246**, 527 (1986).
35. Tektronix model TK2048M (Tektronix, Inc., Beaverton, OR 97077).
36. R. E. Griffiths, *Adv. Electron. Electron Phys.* **64B**, 483 (1985); D. H. Lumb, G. R. Hopkinson, A. A. Wells, *ibid.*, p. 497.
37. V. Duchenois, M. Fouassier, C. Piaget, *ibid.*, p. 365.
38. H. E. Huxley, A. R. Faruqi, J. Bordas, M. H. J. Koch, J. R. Milch, *Nature (London)* **284**, 140 (1980).
39. G. Suarez *et al.*, *Proc. Natl. Acad. Sci. U.S.A.* **82**, 4693 (1985).
40. J. Bordas, E-M. Mandelkow, E. Mandelkow, *J. Mol. Biol.* **164**, 89 (1983).
41. A. Mahendrasingam *et al.*, *Science* **233**, 195 (1986).
42. G. Mulhaupt, *Nucl. Inst. Methods* **A246**, 845 (1986).
43. I am grateful to U. Arndt, D. Bilderback, M. Caffrey, S. Doniach, P. Eisenberger, K. Hodgson, H. Huxley, K. Moffat, G. T. Reynolds, and D. Ringe for comments and references. Biomedical research and instrumentation development in our laboratory is supported by NIH grant GM32614, and DOE grant DE-FG02-87ER60522.A000. Instrumentation development for beam line X-9 at the NSLS is supported by NSF grant PCM 8313069. Research at NSLS beam line X-10 is also supported in part by Exxon Research & Engineering Co.

New Opportunities in Synchrotron X-ray Crystallography

C. T. PREWITT, P. COPPENS, J. C. PHILLIPS, L. W. FINGER

Several high-intensity synchrotron x-ray sources have been constructed over the past few years in the United States, West Germany, Great Britain, Japan, France, Italy, and the Soviet Union. Crystallographers have begun to use these facilities for experiments that take advantage of the characteristics of synchrotron radiation, namely, a broad distribution of wavelengths, high intensity, low divergence, strong polarization, and a pulsed time structure. In addition to more familiar diffraction experiments on single crystals and powdered samples, new types of crystallographic studies, for example, energy-dispersive and surface diffraction studies, have progressed rapidly with more general accessibility of synchrotron sources. These high-intensity sources allow diffraction experiments to be performed on very small crystals or on large biological molecules, and permit weak magnetic scattering to be detected. Anomalous dispersion experiments can exploit the ability to vary the wavelength of the radiation, and the pulsed time structure of the beam makes possible fast time-resolved experiments. Because of the availability of synchrotron x-radiation, these and other kinds of experiments will be in the forefront of crystallographic research for the next several years.

THE TRADITIONAL SOURCE OF INCIDENT RADIATION FOR X-ray diffraction experiments has been an evacuated tube that contains a cathode and anode that is subjected to a high electrical potential. These tubes have been incorporated into a variety of instruments found in laboratories all over the world. In recent years, however, crystallographers have been presented with an extraordinary opportunity resulting from the construction of several high-intensity synchrotron x-ray sources in the United States, West Germany, Great Britain, Japan, France, Italy, and the Soviet Union. Synchrotron radiation results when high-energy electrons are accelerated in the magnetic fields required to close the orbits in storage rings or synchrotrons; for the facilities discussed here, the radiation can have energies ranging from the x-ray into the infrared regions. A typical installation consists of a linear electron accelerator from which electrons are injected at a relatively high energy into a storage ring several tens of meters in diameter. Such a ring consists of straight and curved sections. Electrons are guided around this ring with a series of magnets, and accelerating fields are supplied by one or more radio-frequency (rf) stations located at

---

C. T. Prewitt and L. W. Finger are at the Geophysical Laboratory, Carnegie Institution of Washington, 2801 Upton Street, NW, Washington, DC 20008. P. Coppens and J. C. Phillips are at the Department of Chemistry, State University of New York, Buffalo, NY 14214. J. C. Phillips is also associated with the SUNY X3 beamline, National Synchrotron Light Source, Brookhaven National Laboratory, Upton, NY 11973.

points around the ring. X-radiation is produced and extracted for experimental purposes at bending magnets on curved sections of the ring or at various kinds of insertion devices on the straight sections. These insertion devices are multipole magnets that change the energy distribution of the radiation from that produced by the bending magnets. The fundamental characteristics of synchrotron radiation are a broad distribution of wavelengths, high intensity, low divergence, strong polarization, and a pulsed time structure. In contrast, a conventional x-ray source has most of its relatively low intensity concentrated in characteristic line spectra and is a divergent, unpolarized source with no particular time structure.

In the United States, x-ray synchrotron sources are operating at the Stanford Synchrotron Radiation Laboratory (SSRL), Cornell High Energy Synchrotron Source (CHESS), and National Synchrotron Light Source (NSLS), Brookhaven National Laboratory (BNL). Crystallographers are also using similar sources for x-ray diffraction studies in other countries, most notably at DESY (Deutsches Elektronen Synchrotron) in Hamburg, West Germany, SRS (Synchrotron Radiation Source) in Daresbury, United Kingdom, and the Photon Factory in Tsukuba Science City, Japan.

Each of the characteristics of synchrotron radiation impacts upon experiment design. The broad wavelength distribution allows selection of radiation near absorption edges, and thus anomalous dispersion experiments can be performed. Furthermore, studies can be conducted with either monochromatic or polychromatic beams. The high intensity permits measurement of weak effects such as thermal diffuse scattering, elastic and nuclear Bragg scattering, and satellite reflections. Diffraction data can also be obtained from small crystals with the added benefit that the effects of extinction will be minimized. The low beam divergence yields high intrinsic collimation, high resolution, and high signal-to-noise ratios. Thus features near the main diffraction peaks or those caused by twinned crystals can be resolved. Polarization of the incident beam affects the designs of x-ray optics and diffractometers, improves signal-to-background ratios, and allows discrimination between electronic and magnetic scattering. The pulsed time structure, which results from the grouping of the electrons in the storage ring by the rf system that replaces the radiated energy, allows fast time-resolved experiments and discrimination between electronic (prompt) and nuclear (delayed) scattering.

Today, crystallography covers a broad spectrum of theory and experiment related to both the crystalline and noncrystalline states of matter. This article reviews how crystallographers are using x-ray diffraction and x-ray scattering to explore crystalline structure.

Instrumentation

The characteristics of synchrotron radiation not only provide experimental opportunities but also present challenges in instrumentation. For example, new types of x-ray optics have been developed to monochromatize and focus the beam. Table 1 lists characteristics of diffractometer stations in the United States that are suitable for crystallographic experiments. Optics, detectors, and other instrumentation issues are discussed below.

X-ray optics. A variety of different optical configurations are used for crystallographic experiments at synchrotron sources. The simplest of these consists of a sample in an unconditioned white beam. Energy-dispersive studies, in which diffraction patterns of materials are measured as a function of energy at fixed scattering angles, are typically done this way. At CHESS, the Laue technique is used for time-resolved studies on macromolecules, with moving film as a detector. To avoid overlap from higher order reflections at shorter wavelengths, a band of the spectrum is obtained by the use of attenuators or multilayers and a mirror (*1*).

A typical diffractometer system used on a synchrotron beamline is shown schematically in Fig. 1. The most commonly used optics are a combination of a tunable double-crystal monochromator with a bent toroidal or ellipsoidal double-focusing mirror. The mirror typically gives a 1:1 x-ray image of the electron-beam cross section; magnifications significantly different from 1:1 are difficult to achieve. Silicon or germanium crystals are usually used as monochromators and give bandwidths of the order of 2 eV at 8 keV. The first such beamline at SSRL (*2*) had the mirror as the first optical element and the monochromator near the sample. When first used

Table 1. Synchrotron radiation diffractometers in the United States. The table is restricted to four-circle diffractometers. SSRL, CHESS, and NSLS have 28 other stations devoted to crystallography and diffraction measurements by rotation camera, powder diffraction, surface diffraction, and high-resolution scattering techniques. These laboratories all provide detailed descriptions of their facilities on request. Abbreviations: E, experimental measurement; T, theoretical; F, focused; U, unfocused; HHMI, Howard Hughes Medical Institute; LASL, Los Alamos Scientific Laboratory; ORNL, Oak Ridge National Laboratory; NRL, Naval Research Laboratory.

Laboratory Station Operator	Optics	Focus ($4\sigma_{h,v}$ (mm) Flux (photons/sec) Wavelength (Å)	Wavelength range (Å)	Critical source wavelength (Å)
SSRL (*3*) I-5* SSRL	Nonfocusing two-crystal monochr.		3.3–0.4 U	2.1
CHESS (*74*) A2* CHESS	Nonfocusing two-crystal monochr.§		1.0–0.1 U	0.4
NSLS (*8*) X3A1‡ SUNY	Sideways-focusing monochr.‖	0.4×2.0 1.0×10^{11} 0.655 T	0.655 F	2.5
NSLS (*6*) X3A2* SUNY	Monochr./toroidal mirror¶	1.5×1.0 3.5×10^{11} 2.0–1.4 E	3.5–1.3 F 3.5–0.4 U	2.5
NSLS X4‡ HHMI	Sagittal monochr.			
NSLS (*8*) X7A* BNL Physics	White beam or monochr.#	5.0×2.5 5.0×10^{13} 1.3 T	2.5–0.8 W 2.5–0.6 M	2.5
NSLS (*8*) X7B* BNL Chemistry	Monochr./toroidal mirror**	1.5×1.0 6.0×10^{11} 1.3 T		2.5
NSLS (*8*) X8A‡ LASL	Monochr./toroidal mirror††			2.5
NSLS (*8*) X10A* Exxon	Toroidal mirror/monochr.	1.5×1.0 3.0×10^{11} 1.3 T	6.2–0.8 F	2.5
NSLS (*8*) X10B† Exxon	Flat mirror bent sideways monochr.	1.0×1.0 2.0×10^{11} 1.1 T	1.9–1.1 F	2.5
NSLS (*7, 10*) X14A* ORNL	Flat mirror sagittal monochr.	1.5×1.0 3.0×10^{11} 1.5 E	6.2–0.3 F	2.5
NSLS (*8*) X17B1‡ NSLS	Two-crystal monochr.‡‡			0.5
NSLS (*8*) X23B‡ NRL	Monochr./toroidal mirror‡‡			2.5

*Operating. †Commissioning. ‡Under construction. §Wiggler sagittal focus tested. ‖Monochr. fixed 2θ of 12°. ¶Moved from port X21A. #Moved from port X13A. **Moved from port X13B. ††Flat mirror before monochr. ‡‡Superconducting wiggler.

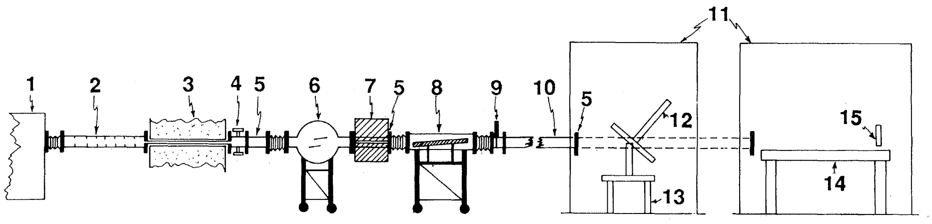

Fig. 1. Schematic drawing of a diffractometer system used with synchrotron radiation (SUNY X21A beamline). Components: 1, front end; 2, acoustic delay line; 3, wall and wall piece; 4, tee piece and sensors; 5, beryllium windows; 6, monochromator; 7, lead collimator; 8, mirror; 9, photon shutter; 10, beam pipe; 11, hutches; 12, 4-θ goniometer; 13, *xyz* table; 14, optical bench; and 15, linear detector.

with a single-crystal diffractometer (*3*), this arrangement allowed the use of broader bandwidth optics, that is, a pair of graphite crystals that gave more flux for experiments in which energy resolution was not important. However, the focusing action of the mirror degraded the energy resolution of the monochromator at shorter wavelengths. Anomalous dispersion measurements at the cesium L edges successfully resolved all of the near-edge features. For the gadolinium L edges, spectroscopy measurements predicted large anomalous dispersion effects (*4*) that were not fully resolved by crystallographic measurements until a nonfocusing, high-energy-resolution beamline was used (*5*). For beamlines with a monochromator as the first element, high energy resolution with focusing can be achieved (*6*), but the ability to use broad-bandwidth optics is lost as the monochromator increases the beam divergence. For either configuration, a short-wavelength cutoff imposed by the mirror limits the available focused spectrum but does serve to eliminate monochromator harmonics. At the high-brightness NSLS x-ray ring, mirrors give an image somewhat larger than the small source size (*7, 8*), possibly because of surface roughness (*9*).

Double-crystal monochromators have heating problems because of the high thermal load on the first crystal and the cycling of the load as the current in the storage ring decays and is replenished. For x-rays to pass through the monochromator, the narrow rocking curves of both crystals must be matched. A small temperature change can shift the curve of the first crystal significantly, which can lead to focal-spot blowup and movement, loss of intensity, and wavelength instability. However, careful cooling and feedback can minimize these problems (*6*). Mirrors in white beams can also have similar problems.

Double-crystal monochromators with the second crystal bent about an axis parallel to the x-ray beam [sagittal focusing (*10*)] should solve some of the problems associated with mirrors and monochromators. There is no intrinsic wavelength cutoff, and a greater range of magnifications is possible. There should be no surface roughness effects to blur the focus, but progressive inefficiency with shorter wavelength results in a cutoff at ~0.6 Å. At NSLS inexact bending coupled with heat loading has led to focal spots that are no smaller than those achieved with mirrors. Only the horizontal spread is focused. The NSLS setup uses a flat mirror for vertical focusing (*11*).

A different type of focusing is achieved with the sideways-diffracting triangular monochromator bent around a vertical axis perpendicular to the x-ray beam (*12*). This uses only one crystal and thus has no wavelength limitation and is less subject to thermal problems. Magnification is variable, but tuning the wavelength causes the beam to sweep sideways so that realignment is often necessary. Under special conditions a narrow-bandwidth beam suitable for anomalous dispersion studies may be obtained (*13*). The source-monochromator-focus distances must be varied during tuning for narrow-bandwidth work. In an overbent configuration and with an area detector, simultaneous polychromatic data collection is possible (*14*). A single sagittally bent monochromator has been proposed to combine the best features of the latter two monochromators for use with short-wavelength sources (*15*).

Apart from graphite, candidates for wide-bandwidth monochromators include large single crystals of elements with high atomic numbers such as cadmium telluride and multilayers; the latter are layered structures of alternating vapor-deposited elements, for example, tungsten and silicon. At NSLS, multilayers used in small-angle scattering experiments gave an order of magnitude flux increase over Si(111) crystals (*16*). At SSRL, two spherical multilayers were used in a Kirkpatrick-Baez geometry to produce a microfocus of ~1.5 Å radiation (*17*). Such optics could also prove useful in crystallography, and it should be possible to extend the useful wavelength range.

Diffractometers. Most diffractometers in use with synchrotron radiation are similar to conventional diffractometers, except that they are mounted sideways with the crystal (ω) and detector (θ) rotation axes horizontal, as are the axes of diffracted-beam monochromators when they are used. This type of mounting avoids diffracted intensity losses due to the polarization of the synchrotron radiation beam. A type of diffractometer incorporated into many different beamlines at different storage rings is shown in Fig. 2. At the Photon Factory, a vertical wiggler with horizontal polarization is used as a source for a conventionally oriented diffractometer (*18*). Whatever the diffractometer orientation, a carriage is necessary to bring it into alignment with the incident beam (*3*).

Some diffractometers have more unusual geometries and capabilities. The multipurpose two-axis diffractometer at Hamburger Synchrotron Strahls Labor (HASYLAB) (*19*) was built especially for synchrotron radiation diffraction so that the angle between the polarization plane of the beam and the ω-θ axis can be selected. Its construction permits many types of scattering, diffraction, and crystallography experiments to be performed. The NSLS X7A diffractometer can swing to a position where the monochromator is in a backscattering configuration. For magnetic scattering, an exit beam monochromator with a second out-of-plane reflection was used to discriminate between magnetically and electronically scattered photons (*20*).

Film cameras. Most macromolecular data collection has used film as a detector. The original work used a precession camera, which has the advantages of allowing selection of reciprocal lattice planes for trial experiments and of not needing incident beam monitoring (*21*). The vast majority of studies since have used rotation cameras (*22*). These devices need alignment carriages and usually have small ion chambers as beam monitors (*23*). Of special note is the multifunction setup at Daresbury, United Kingdom, where the camera can be fed either by wiggler magnet radiation as a white beam, from a double-crystal monochromator, or from a sideways-diffracting monochromator (*24*).

Detectors. White-beam energy-dispersive work has typically used Si(Li) or intrinsic germanium energy-discriminating detectors, sometimes with time-resolved capability. These detectors are particularly good for measuring diffraction patterns of polycrystalline materials as a function of temperature or pressure and have been used successfully to monitor phase transitions as environmental conditions are varied.

Monochromatic-beam diffractometry typically uses standard NaI(Tl) detectors that can be equipped with time-resolved readout (*25*). Linear position-sensitive detectors have been used with conventional systems to speed up data collection (*26*) and also with synchrotron radiation diffractometers for time-resolved work (*27*). Two-dimensional detection systems are in use for anomalous dispersion studies of proteins (*28*), and other systems are planned. All of these linear and area detectors are gas-filled proportional detectors. New types of detectors, for example, photodiodes (*16*) and laser-stimulated luminescence readout (*29, 30*), are becoming available.

The diffracted-beam intensities must be normalized to the decaying incident beam. Ion chambers in the beam or NaI(Tl) detectors that monitor scattered radiation from a thin film in the beam are usually used.

Sample environments. Low-temperature devices have been used at CHESS and NSLS (*31*) in crystallographic studies. Both systems use closed-cycle cryostats at liquid helium temperature that are supported in the diffractometer by alignment slides that were installed by the diffractometer manufacturers, and a rotating-seal pivot arm that was devised at CHESS. Full rotation about the crystal rotation axis (ϕ) and the full circle (χ) is possible, thus allowing access to a large volume of reciprocal space.

High-temperature furnaces have been used in conventional x-ray diffraction experiments for many years (*32*). All of the advantages of synchrotron radiation mentioned above also apply in high-temperature experiments, although most studies have been done in connection with high-pressure work. Two approaches have been used to obtain high pressure while enabling the experimenter to x-ray a sample. With the diamond-anvil cell (*33*) a single-crystal or polycrystalline sample is held at high pressure between two diamonds and the x-rays are directed through the diamonds and the sample. With the cubic-anvil device six tungsten carbide pistons press on the faces of a cube containing a polycrystalline sample. Such a device (MAX-80) has been used successfully at the Photon Factory for several years (*34*). Investigators have been able with both types of apparatus to heat samples while irradiating and maintaining them at high pressure (*35*).

Software

Since digital computers and counter diffractometers first became available, crystallographers have developed many sophisticated diffractometer control programs. These programs can be used with synchrotron diffractometers after relatively minor modifications and additions. In addition to the diffracted beam intensity record, information from the main beam monitor and other beamline devices such as beam position monitors can be stored and used in data reduction. The collimation of the synchrotron radiation beam produces narrow reflections from nonmosaic sample crystals (*3*) that are best centered by special routines (*5*). The narrow reflections can also produce problems with search routines and crystal alignment photographs. Because beamline time at a synchrotron radiation facility is limited, graphics packages to examine peak profiles rapidly, to check peak centering, and to monitor the intensity data are important. Other programs provide automatic alignment and monochromator calibration routines (*36*). Preliminary data reduction programs need only be modified to include the beam decay correction and the appropriate polarization correction. The degree of polarization of the beam at the sample position can be measured readily with specially designed devices (*37*).

Applications

The time structure of the synchrotron beam can be used for time-resolved experiments on a nanosecond time scale. Time-resolved diffraction experiments are described elsewhere in this issue (*38*) and thus are not discussed here.

Comparison of the intensity of the synchrotron beam with that available at a conventional source is not straightforward, because the synchrotron beams have much lower divergence, which is of greater benefit when working with a low mosaic spread crystal. For crystals with a mosaic spread of about 0.05° to 0.25°, a factor of 1000 gain is typically obtained at a bending-magnet beamline. The high intensity of synchrotron radiation allows small crystals of ~10-μm linear dimension to be used as samples, although mounting such a crystal on a suitably sized support is by no means trivial and requires further development. One of the first demonstrations of the use of small crystals was carried out by Bachman *et al.* (*39*), who used a 6-μm CaF_2 crystal to measure a complete set of diffraction intensities at DESY. More recent applications have involved zeolites, catalytically important minerals that are not generally available as single crystals of the size required with conventional sources. Kvick and Rohrbaugh have studied borosodalite (*40*), a zeolite in which some of the aluminum atoms have been replaced by boron. They used a crystal with an edge size of 50 μm and noted that a considerably smaller crystal could have been used. These techniques have eliminated a barrier in the study of zeolites and the chemistry of their cavities, because previously there was a range of particle sizes, ~5 to 80 μm, that could not be treated satisfactorily with either single-crystal or powder diffraction techniques.

Solid and liquid surface structure. The small number of atoms participating in the scattering process is particularly pronounced for surfaces, for which diffraction studies have been greatly facilitated with the advent of synchrotron radiation, thus opening a completely new field of two-dimensional x-ray crystallography. Whereas a 100-μm crystal may contain 10^{17} atoms, the number of atoms in a 10-Å-thick surface layer of the same linear dimension of 100 μm will be three orders of magnitude smaller. Surface scattering can be enhanced, however, by using a grazing angle of incidence (*41*). When

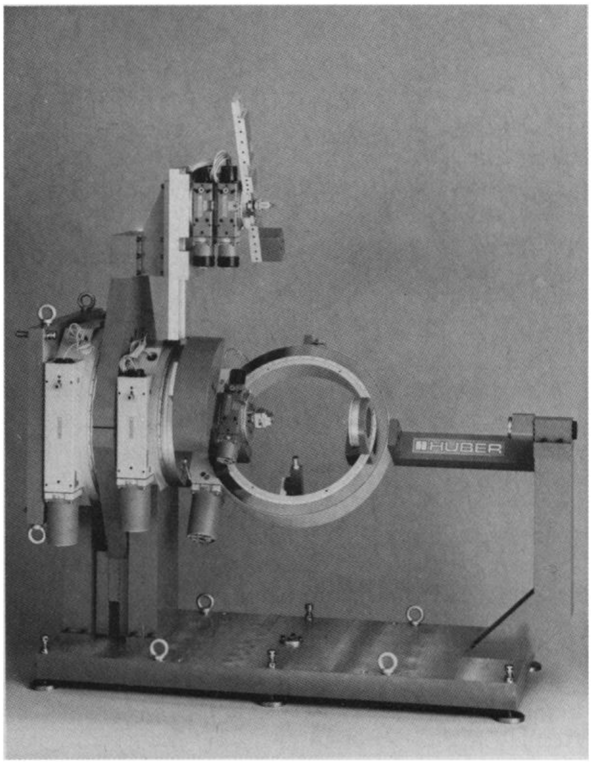

Fig. 2. Photograph of a diffractometer designed for work with synchrotron radiation. The goniometer is supported by a frame that maintains the ω-θ axis in a horizontal position so that diffraction patterns can be measured in a vertical plane. [Photo courtesy of Huber Diffraktionstechnik GmbH and Blake Industries, Inc.]

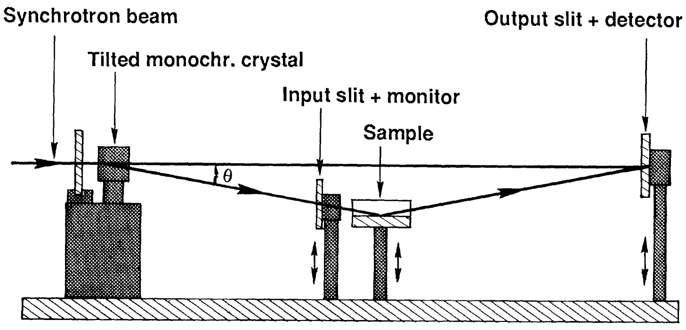

Fig. 3. Experimental arrangement for x-ray surface studies [adapted from (*43*)].

a beam is incident on a sample at or below the angle of total reflectance, it only penetrates about ten atomic layers into the crystal and continues to travel along the surface. The scattering of this evanescent beam takes place along a considerable path length, which increases the diffracted intensity. A diagram of an experimental arrangement for the study of liquid surfaces (*42, 43*) is shown in Fig. 3.

Because many chemical and biological processes occur at interfaces, such structural knowledge is of enormous importance. In many atomic solids, the surface structure differs from the bulk structure in the absence of some of the atoms. Such reconstructed surfaces typically have longer repeat distances than the equivalent dimension in bulk. Examples that have been studied include the (001)-(2 × 1) reconstructed surface of germanium (*41*), the (111)-(7 × 7) reconstructed surface of silicon (*44*) [which is the first known example of a reconstructed surface, having been discovered in 1959 (*45*), but which is still not fully understood]; the reconstructed (110)-(2 × 1) surface of gold in which every second row of atoms is missing (*46*), and the (111)-(2 × 2) surface of InSb (*47*). In the last study Patterson techniques, which are widely applied in bulk crystallography, were used for the first time to directly determine a surface structure, which in this case was a distortion of the bulk structure with probably slightly longer bond lengths.

Modification of surfaces by amorphous or epitaxial overlayers can also be investigated. Robinson *et al.* (*44*) described the change in silicon surface structure brought about by deposition of an amorphous layer (*48*), whereas Zegenhagen *et al.* (*49*) studied the lattice mismatch between a Si(111) surface and an epitaxial layer of $NiSi_2$ as a function of the thickness of the epitaxial layer. The mismatch between the overlayer and the substrate induces elastic strain, which results in a slightly distorted lattice unit cell of $NiSi_2$.

Since the discovery of organic monolayers on water (Langmuir films) 70 years ago, only indirect evidence on positional order and melting transitions has been available. This situation has now changed dramatically. Studies of lead stearate on water (*50*), of phospholipid monolayers (*51*), and of the surfactant palmitoyl-(*R*)-lysine on water (*52*) have been reported. The last study shows the packing arrangement of the amino acid head groups to be very close to that found in α-glycine and several hydrophobic amino acids, and explains why the monolayer at the air-water interface induces epitaxial nucleation of these amino acids in water.

Crystallography and physical properties. Several weak, but important, physical effects have become accessible with synchrotron x-radiation. Because x-rays are part of the electromagnetic spectrum, they interact with the magnetic as well as the charge distribution in a solid. However, the ratio of the intensity of the two types of scattering is about 10^5, with the magnetic scattering being weaker. This disadvantage is compensated by the unusual intensity of the synchrotron beam. It allows determination of the magnetic structure and, unlike magnetic scattering by neutrons, allows the separation of orbital and electron-spin scattering through analysis of the polarization dependence of the photon beams. A study on holmium metal has been reported, and recent theoretical studies indicate that it will be possible to distinguish between magnetic scattering from spin and orbital angular momentum in ferro- and antiferromagnets (*53*).

Application of a polarizing electric field to dielectric materials leads to small but measurable changes in x-ray scattering. A program to investigate such changes has been started by Kvick *et al.* at NSLS (*25*). Initial studies have been made on the ferroelectric material $LiNbO_3$, in which changes in intensity and position of the Bragg peaks at a field of 30 kV/cm have been observed. The difference between peak intensities with field up and field down decreases dramatically when the frequency of the applied field is increased above 150 Hz. There is also a difference in behavior between the bulk material and the region at the electrode-crystal interface. A second study concerns the nonlinear optical material 2-methyl-4-nitroaniline, which is used in second-harmonic generation (frequency doubling) (*54*). In this material the dependence on the frequency of the applied field is absent. The difference between the field up and field down intensities is small but measurable (Fig. 4). Analysis of the data indicates that both molecular polarizability and molecular reorientation contribute to the intensity changes. The effect allows, for the first time, mapping of the shift of electron density at the molecular level.

Another effect that is too weak to quantify with conventional sources is related to metal-insulator transitions that occur on cooling of low-dimensional solids. The distortions that occur in the crystals at the transition temperature cause weak satellite reflections. Analysis of the intensities of such reflections for the organic conductor TTF-TCNQ (tetrathiofulvalene-tetracyanoquinodimethane) at 15 K allows the derivation of the molecular displacements responsible for the disappearance of electrical conductivity (*31*). The solids are built up of one-dimensional stacks of molecules, along which conductivity occurs. A curious result is that stacks, which are equivalent in the high-temperature structure, distort in nonequivalent ways and thus create a different electronic band gap for chemically equivalent stacks.

Application to chemical and biological samples. That the synchrotron beam may also be used for highly accurate studies has been demonstrated through measurement of the charge distribution in an inorganic complex (*55*). Such measurements require as high an accuracy as can be achieved, because small shifts in the electron density due to chemical bonding need to be determined. The short wavelengths available at some synchrotron sources have the advantage of reducing or eliminating effects that limit the accuracy of the diffraction measurements such as absorption and extinction. The quality of the density maps obtained for the complex chromiumhexamine-hexacyanochromium at a wavelength of 0.302 Å shows that synchrotron radiation offers significant advantages for such precise measurements (*55*).

The synchrotron beam can be tuned over a wide wavelength range to exploit changes in the scattering power of specific atoms. The real and imaginary components of the atomic scattering factor show large variations near the atomic absorption edges, particularly at the *L* edges. Templeton and co-workers (*56*) have shown, for example, that the cesium atom in cesium hydrogen(+)tartrate shows an unprecedented decrease in scattering power of -27.1 ± 9 electrons at the L_3 edge. Such effects offer a substitute for the isomorphous replacement method in protein crystallography and may eliminate the need for obtaining several isomorphous derivatives in the phase-determination process (*57*). Studies on a ferrodoxin (*58*) and on sulfite reductase (*59*) with this technique have been reported. In both cases the data were collected with a two-dimensional area detector, each frame of data being measured sequentially at four or

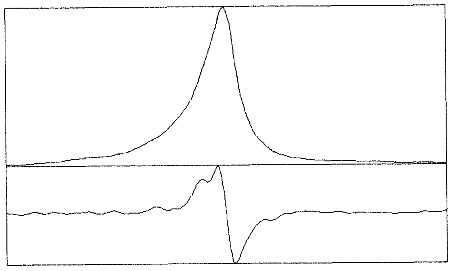

Fig. 4. Plot of intensity versus angle for total scattering (**top**) and difference scattering (**bottom**) (×42.7) of the $h,k,l = 4,0,\bar{6}$ reflection of a crystal of 2-methyl-4-nitroaniline subjected to external fields of +106 and −106 V/m; voltage, 1000 V; frequency, 35 Hz; scan width, 0.8000; maximum intensity (I_{max}), 169981; dI_{max}, 2497; I_{mean}, 4034343; dI/I, 0.2624%. The lower curve is the difference between the scattering with field up and field down.

five wavelengths. This procedure is made possible by the ease of changing wavelengths at a synchrotron beam equipped with a fixed exit-beam monochromator. A membrane study of bacteriorhodopsin titrated with terbium has also been reported (*60*). An early application of the variation of atomic scattering factor near an absorption edge is the determination of cation site occupancy in disordered cobalt ferrite by Yakel (*61*).

In environments with pronounced anisotropy, the change in scattering power near the atomic absorption edge may be dependent on the direction of the electric vector of the polarized photon beam. Such dichroism has been measured in crystals of vanadyl bisacetyl acetonate (*62*), rubidium uranyl nitrate (*63*), and sodium bromate (*64*). In the vanadyl compound all molecules are either parallel or antiparallel. A sharp anisotropic absorption occurs near the *K* absorption edge of vanadium (a "white line"), which is due to the excitation of a 1*s* electron into a vacant molecular orbital. Under such conditions rules for absence of reflections due to screw axes and glide planes are no longer rigorous. The effect can be used for selectively determining the positions of the anisotropically scattering atoms in crystals (*65*).

A tremendous advantage of the synchrotron beam in macromolecular crystallography is that the time span for collection of a large data set may be reduced from months or even years to days or hours. Very small crystals may be used (~50 μm), and sensitivity to radiation is reduced because of the shorter exposure time. The small size of the beam and its collimation allow resolution of reflection maxima of crystals with very large unit cells. Collection of viruses with unit cells as large as 1000 Å (~10,000,000 daltons) has become possible (*16*). For example, the atomic structure of mengo virus at 3.0 Å resolution was determined by Rossmann and coworkers (*67*). This virus has a unit cell with a linear dimension of ~450 Å. High-quality photographic data were collected at CHESS by the rotation technique with a different crystal for each of 600 1-minute exposures. The same method was used in the analysis of human rhino (common cold) virus (*67*) and its complexes with two antiviral agents (*68*). Relations between these and other structures give insight into the evolution of viruses and their interaction with drugs and other chemical substances.

Powder diffraction. The extremely high resolution made possible because of the small beam divergence and the use of perfect single crystals as monochromators has added new capabilities for x-ray diffraction studies of powders. Powder diffraction data have been used extensively for phase identification and in recent years for the refinement of known crystal structures with the Rietveld technique (*69*). It has been difficult, however, to determine the small splitting of diffraction lines associated with slight deviations from an ideal symmetry. Consequently, most attempts to determine an unknown crystal structure have required a single crystal.

At NSLS, an instrument has been developed that will achieve a resolution corresponding to a full width at half-maximum of 0.02°, as compared with 0.2° that is obtained with a conventional diffractometer (*70*). With such an instrument, it is possible to extract integrated intensities from the pattern and to use these data to solve an unknown structure with Patterson or other direct structure-solving techniques (*71*). The Rietveld method is then used in the final refinement. This procedure should be extremely valuable in the determination of structures of materials that do not form single crystals even as large as 10 μm.

The polychromatic nature of synchrotron radiation is conducive to the use of so-called energy-dispersive analysis. In this technique, a fixed scattering angle is selected and the energy of the scattered radiation is used to determine the magnitude of the scattering vector. Although this technique has rather low resolution ($\Delta E/E \approx 10^{-2}$, where E is energy), it has become important for the study of powders at high pressure in the diamond-anvil cell. In a monochromatic experiment, the sample chamber must not obstruct the incident and diffracted beams. For single-crystal experiments, the open areas must be conical, which limits the maximum pressure to approximately 10 GPa because the diamonds are relatively unsupported. For a powdered sample the incident beam can enter through a hole and the diffracted beam can exit through a narrow slot, which improves the diamond supports and increases the maximum pressure by a factor of 20 or more. With a polychromatic incident beam, it is possible to cover much larger scattering amplitudes than is possible with a monochromatic beam.

Synchrotron radiation is also used to excite the optical ruby fluorescence radiation used for pressure calibration in diamond-cell experiments (Fig. 5). Not only can the pressure be determined

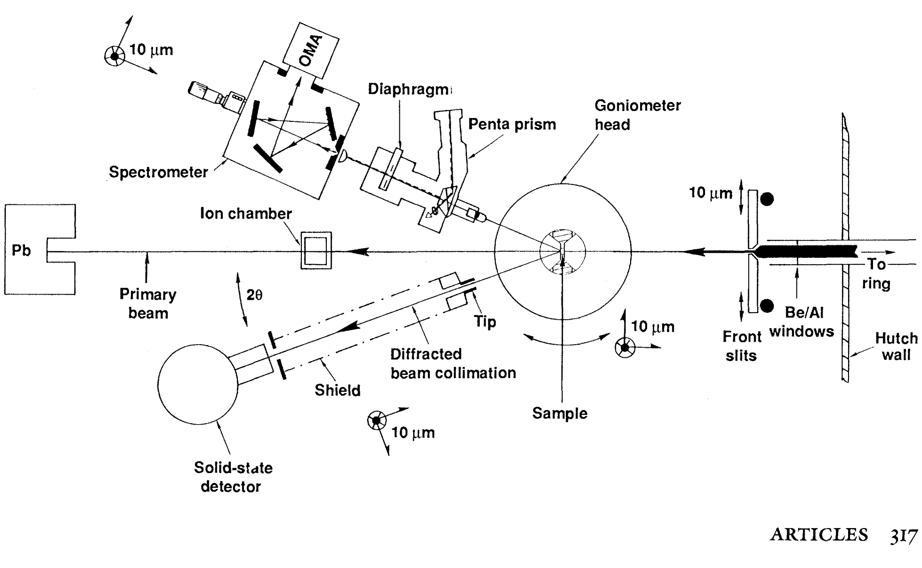

Fig. 5. Plan view of apparatus used for energy-dispersive x-ray diffraction. The lower section consists of the collimators and detectors for the diffracted x-rays. The upper section contains the apparatus used to detect the x-ray–induced ruby fluorescence that is used to determine the pressure, OMA, optical multichannel analyzer.

without dismounting the sample, but the actual pressure of the sample in a pressure gradient can be determined.

The apparatus in Fig. 5 has been used to study ordinary powders such as silicon, iron, and tungsten and the powders formed by the high-pressure crystallization at room temperature of gases such as xenon, neon, O_2, and N_2 (*72*). An interesting experiment resulted from the crystallization of H_2 and D_2 (*73*). These materials formed several small crystals, which were too few in number to yield a powder pattern; therefore, a single-crystal experiment was required. A simple two-circle goniometer was constructed that permitted the scattering vector to be oriented properly and the diffraction pattern for each class of planes to be recorded separately.

Conclusions

Of all experimental techniques used with synchrotron x-rays, crystallographic measurements may place the most stringent demands on the long-term stability of source, optics stability, and detector linearity. It is now 10 years since the earliest single-crystal diffractometry work in which a parasitic beamline with nonoptimal optics was used on a low-brightness storage ring with poor orbit stability. Since then, many improvements and innovations have been made. These improvements were made slowly at first (there was a 7-year gap between the commissioning of the first and second diffractometers), but the rate of commissioning of new experimental stations and novel experiments has risen sharply with the start of operations at NSLS. Intensities, wavelength resolution, and range and focal spot sizes have improved with high-brightness lattices and insertion device beamlines. New insertion devices at NSLS, SSRL [on both SPEAR (Stanford Positron-Electron Accelerating Ring) and PEP (Positron Electron Project)], CHESS, and the proposed Advanced Photon Source at Argonne National Laboratory will undoubtedly have properties that will attract crystallographers. Existing and new sources are a challenge in optics and beamline layout, presenting both experimental opportunities and engineering difficulties.

New types of crystallographic studies, for example, energy-dispersive and surface diffraction studies, are possible now because of the general accessibility of synchrotron sources. The startup of NSLS has also provided more beam time for these studies. In addition, the properties of the new sources have become of interest to theorists and have led to their involvement in helping to design experiments and to interpret the results. It is clear that in the next few years there will be intense activity by crystallographers at synchrotron sources, leading to much progress in the ability to deduce the structure and properties of matter.

REFERENCES AND NOTES

1. D. H. Bilderback, K. Moffatt, D. M. E. Szebenyi, *Nucl. Instrum. Methods Phys. Res.* **222**, 245 (1984); K. Moffatt, D. H. Bilderback, W. Schildkamp, K. Volz, *ibid.* **A246**, 627 (1986).
2. J. B. Hastings, B. M. Kincaid, P. Eisenberger, *Nucl. Instrum. Methods* **152**, 167 (1978).
3. J. C. Phillips, J. A. Cerino, K. O. Hodgson, *J. Appl. Crystallogr.* **12**, 592 (1979).
4. R. C. Lye, J. C. Phillips, D. Kaplan, S. Doniach, K. O. Hodgson, *Proc. Natl. Acad. Sci. U.S.A.* 77, 5884 (1980).
5. L. K. Templeton, D. H. Templeton, R. P. Phizackerley, K. O. Hodgson, *Acta Crystallogr.* **A38**, 74 (1982).
6. P. Coppens, F. S. Nielsen, J. C. Phillips, B. W. Batterman, *Am. Crystallogr. Assoc. Abstr.* **12**, 45 (1984).
7. "National Synchrotron Light Source annual report 1985," *Brookhaven National Laboratory Report 51947*, W. Thomlinson and S. M. White-DePace, Eds. (Brookhaven National Laboratory, Upton, NY, 1986).
8. "Guide to the VUV and x-ray beamlines," *National Synchrotron Light Source Users Manual*, S. M. White-DePace and N. F. Gmur, Eds. (Brookhaven National Laboratory, Upton, NY, 1986).
9. "National Synchrotron Light Source annual report 1986," *Brookhaven National Laboratory Report 52045*, S. M. White-DePace and N. F. Gmur, Eds. (Brookhaven National Laboratory, Upton, NY, 1987).
10. C. J. Sparks, G. E. Ice, J. Wong, B. Batterman, *Nucl. Instrum. Methods Phys. Res.* **194**, 73 (1982).
11. A. Habenschuss, G. E. Ice, C. J. Sparks, R. Neiser, *ibid.*, in press.
12. M. Lemmonier, R. Fourme, F. Rousseaux, R. Kahn, *Nucl. Instrum. Methods* **152**, 173 (1978).
13. G. Rosenbaum and K. Holmes, in *Synchrotron Radiation Research*, H. Winick and S. Doniach, Eds. (Plenum, New York, 1980), pp. 533–564.
14. U. W. Arndt *et al.*, *Nature (London)* **298**, 835 (1982).
15. J. C. Phillips, in *Structural Biological Applications of X-ray Absorption, Scattering and Diffraction*, H. D. Bartunik and B. Chance, Eds. (Academic Press, Orlando, FL, 1986), pp. 357–365.
16. G. B. Stephenson, *Nucl. Instrum. Methods Phys. Res.*, in press.
17. A. C. Thomson, Y. Wu, J. H. Underwood, T. W. Barbee, Jr., *ibid.* **A255**, 603 (1987).
18. T. Yamakawa *et al.*, *ibid.* **A246**, 32 (1986).
19. U. Bonse and K. Fischer, *ibid.* **190**, 593 (1981).
20. D. E. Moncton, D. Gibbs, J. Bohr, *ibid.* **A246**, 839 (1986).
21. J. C. Phillips, A. Wlodawer, M. M. Yevitz, K. O. Hodgson, *Proc. Natl. Acad. Sci. U.S.A.* **73**, 128 (1976); J. C. Phillips *et al.*, *Acta Crystallogr.* **A33**, 445 (1977).
22. H. D. Bartunik, R. Fourme, J. C. Phillips, in *Uses of Synchrotron Radiation in Biology*, H. B. Stuhrmann, Ed. (Academic Press, London, 1982), pp. 145–202; J. R. Helliwell, *Rep. Prog. Phys.* **47**, 1403 (1984); J. R. Helliwell, *J. Mol. Struct.* **130**, 63 (1985).
23. H. D. Bartunik, P. Clout, B. Robrahn, *J. Appl. Crystallogr.* **14**, 134 (1981).
24. J. R. Helliwell *et al.*, *Nucl. Instrum. Methods Phys. Res.* **A246**, 617 (1986).
25. A. Kvick, E. M. Chen, K. Stahl, S. C. Abrahams, in (*9*), p. 341.
26. E. Prince, A. Wlodawer, A. Santoro, *J. Appl. Crystallogr.* **11**, 173 (1978).
27. H. D. Bartunik, *Rev. Phys. Appl.* **19**, 671 (1984).
28. R. Kahn, R. Fourme, R. Bosshard, V. Saintagne, *Nucl. Instrum. Methods Phys. Res.* **A246**, 596 (1986); R. P. Phizackerley, C. W. Cork, E. A. Merritt, *ibid.*, p. 579.
29. J. Miyahara, K. Takahashi, Y. Amemiya, N. Kamiya, Y. Satow, *ibid.*, p. 572.
30. Y. Amemiya *et al.*, *Science* **237**, 164 (1987).
31. P. Coppens *et al.*, unpublished results.
32. G. E. Brown, S. Sueno, C. T. Prewitt, *Am. Mineral.* **58**, 698 (1973).
33. R. M. Hazen and L. W. Finger, *Comparative Crystal Chemistry: Temperature, Pressure, Composition and the Variation of Crystal Structure* (Wiley, New York, 1982); W. A. Bassett, M. D. Furnish, E. Huang, in *Solid State Physics under Pressure: Recent Advances with Anvil Devices*, S. Minomura, Ed. (Kluwer Academic, Norwell, MA 1985), pp. 335–341; E. F. Skelton, S. B. Qadri, W. T. Elam, A. W. Webb, *ibid.*, pp. 329–334.
34. O. Shimomura *et al.*, *ibid.*, pp. 351–357.
35. M. Manghnani *et al.*, *ibid.*, pp. 343–350; K. Tsuji *et al.*, in *Photon Factory Activity Rep.* (Photon Factory, Tsukubta Science City, Japan) **4**, 285 (1986).
36. At NSLS, a crystallography subgroup of the Users Organization has served as a body through which a neutron diffractometer program was distributed for development for synchrotron radiation use. Four NSLS systems use or plan to use programs with this core, as does the CHESS A2 station.
37. G. Materlik and P. Suortti, *J. Appl. Crystallogr.* **17**, 7 (1984); J.-L. Staudenmann, L. D. Chapman, W. J. Murphy, G. L. Liedl, *ibid.* **18**, 519 (1985).
38. S. M. Gruner, *Science* **238**, 305 (1987).
39. R. Bachman *et al.*, *Angew. Chem. Int. Ed. Engl.* **22**, 1011 (1983).
40. A. Kvick and W. J. Rohrbaugh, in (*9*), p. 340.
41. W. C. Marra, P. Eisenberger, A. Cho, *J. Appl. Phys.* **50**, 6927 (1979); P. Eisenberger and W. C. Marra, *Phys. Rev. Lett.* **46**, 1081 (1981).
42. P. Fuoss and I. K. Robinson, *Nucl. Instrum. Methods Phys. Res.* **222**, 171 (1984).
43. J. Als-Nielsen and P. S. Pershan, *ibid.* **208**, 545 (1983).
44. I. K. Robinson, P. Fuoss, J. Stark, P. A. Bennett, in (*7*), p. IX-102.
45. R. E. Schillier and H. E. Farnsworth, *J. Chem. Phys.* **30**, 917 (1959).
46. I. K. Robinson, *Phys. Rev. Lett.* **50**, 1145 (1983).
47. J. Bohr *et al.*, *ibid.* **54**, 1275 (1985).
48. I. K. Robinson, W. K. Waskiewicz, R. T. Tung, J. Bohr, *ibid.* **57**, 2714 (1986).
49. J. Zegenhagen *et al.*, unpublished results.
50. P. Dutta *et al.*, *Phys. Rev. Lett.* **58**, 2228 (1987).
51. M. Seul, P. Eisenberger, H. M. McConnell, *Proc. Natl. Acad. Sci. U.S.A.* **80**, 5795 (1983); K. Kjaer, J. Als-Nielsen, C. A. Helm, L. A. Laxhuber, H. Möhwald, *Phys. Rev. Lett.* **58**, 2224 (1987).
52. S. G. Wolf *et al.*, *Nature (London)* **328**, 63 (1987).
53. M. Blume, *J. Appl. Phys.* **57**, 3615 (1985); D. Gibbs, D. E. Moncton, K. L. D'Amico, J. Bohr, B. H. Grier, *Phys. Rev. Lett.* **55**, 234 (1985).
54. A. Paturle, R. M. Wing, V. Petricek, P. Coppens, A. Kvick, *Proceedings of the CHESS User Meeting*, Ithaca, NY, 1987, abstr., p. 65.
55. F. K. Nielsen, P. Lee, P. Coppens, *Acta Crystallogr.*, in press.
56. D. H. Templeton, L. K. Templeton, J. C. Phillips, K. O. Hodgson, *ibid.* **A36**, 436 (1980); J. C. Phillips, D. H. Templeton, L. K. Templeton, K. O. Hodgson, *Science* **201**, 257 (1978).
57. R. Kahn *et al.*, *FEBS Lett.* **17A**, 133 (1971); W. A. Hendrickson, J. L. Smith, S. Sheriff, *Methods Enzymol.* **115**, 41 (1985); W. A. Hendrickson, *Trans. Am. Crystallogr. Assoc.* **21**, 11 (1985).
58. H. M. Krishna Murthy *et al.*, in (*9*), p. 132.
59. D. E. McRee, W. A. Hendrickson, J. A. Tainer, E. D. Getzoff, *ibid.*, p. 130.
60. S. Wakatsuki, K. O. Hodgson, R. M. Stroud, S. Doniach, *ibid.*, p. 148.
61. H. L. Yakel, *J. Phys. Chem. Solids* **41**, 1097 (1980).
62. D. H. Templeton and L. K. Templeton, *Acta Crystallogr.* **A36**, 237 (1980).
63. ———, *ibid.* **A38**, 62 (1982).
64. ———, *ibid.* **A42**, 478 (1986).

65. Ming Luo *et al.*, *Science* **235**, 182 (1987).
66. R. Usha *et al.*, *J. Appl. Crystallogr.* **17**, 147 (1984).
67. M. G. Rossmann *et al.*, *Nature (London)* **317**, 145 (1985).
68. T. J. Smith *et al.*, *Science* **233**, 1286 (1986).
69. H. M. Rietveld, *J. Appl. Crystallogr.* **2**, 65 (1969).
70. D. E. Cox, J. B. Hastings, L. P. Cardoso, L. W. Finger, Materials Science Forum, *High Resolution Powder Diffraction*, C. R. A. Catlow, Ed. (Trans. Tech. Publications, Addermannsdorf, Switzerland, 1986).
71. J. P. Attfield, A. W. Sleight, A. K. Cheetham, *Nature (London)* **322**, 620 (1986).
72. R. J. Hemley *et al.*, in *AIRAPT International High Pressure Conference*, Kiev, U.S.S.R., 1987, Abstr., p. 303.
73. H.-K. Mao *et al.*, *ibid.*, p. 306.
74. J. C. Phillips, K. J. Baldwin, W. F. Lehnert, A. D. LeGrand, C. T. Prewitt, *Nucl. Instrum. Methods Phys. Res.* **A246**, 182 (1986).
75. C.T.P., P.C., and J.C.P. acknowledge the support of DOE grant DE-FG02-86ER45231. L.W.F. acknowledges the support of NSF grant EAR84-19982.

The Role of Protein Structure in Chromatographic Behavior

FRED E. REGNIER

Chromatographic retention is determined by a relatively small number of amino acids located in a chromatographic contact region on the surface of a polypeptide. This region is determined by the mode of separation and the amino acid distribution within the polypeptide. The contact area may be as small as a few hundred square angstroms in bioaffinity chromatography. In contrast, the contact region in ion exchange, reversed phase, hydrophobic interaction and the other nonbioaffinity separation modes is much broader, ranging from one side to the whole external surface of a polypeptide. Furthermore, structural changes that alter the chromatographic contact region will alter chromatographic properties. Thus, although immunosorbents can be very useful in purifying proteins of similar primary structure, they will be ineffective in discriminating between small, random variations within a structure. Nonbioaffinity columns complement affinity columns in probing a much larger portion of solute surface and being able to discriminate between protein variants.

INTERFACIAL PHENOMENA AND SURFACE-SURFACE INTERACTIONS play a key role in the organization and control of biological systems. Gene duplication, enzyme catalysis, hormonal regulation, membrane synthesis, and the organization of multiple enzyme complexes all depend on surface recognition. These highly specific interactions occur only when there is sufficient geometric complementarity between enough groups on the surface of two macromolecules to initiate intermolecular docking. Although docking is driven by weak forces such as hydrogen bonding, electrostatic attraction, and hydrophobic interactions, the total force of interaction is very strong because of the involvement of multiple groups.

In this article, I will show that there is considerable similarity between the variables that direct intermolecular docking in biological macromolecules and those that determine the chromatographic behavior of proteins. On the basis of current knowledge of protein-protein interactions and the fact that proteins are three-dimensional matrices with great diversity in the distribution of surface functional groups, one would predict that (i) it is sterically impossible for all of the amino acid residues to come in contact with the surface of a chromatographic sorbent simultaneously, (ii) only those residues at or near the exterior surface of the protein will have a major impact on chromatographic behavior, (iii) only a fraction of the external amino acid residues interact with a particular type of chromatography matrix, such as an ion-exchange sorbent or bioaffinity matrix, (iv) heterogeneity in the amino acid distribution at the protein surface may allow portions of the external surface to dominate chromatographic behavior, (v) the region of the external surface that determines chromatographic behavior may vary between chromatographic modes, (vi) structural changes in a protein that alter amino acid composition in the solute-sorbent contact region will alter chromatographic behavior, and (vii) the chromatographic matrix could alter the structure of an adsorbed protein. Because the systematic study of variables that control chromatographic behavior of proteins is still in the early stages, these hypotheses can only be considered a preliminary working model. Evidence supporting this model and the implications of the model will be presented below.

Steric Effects

Although logic alone suggests that steric phenomena play a role in the interaction of large molecules with a surface, it is possible to show quantitatively that this is true. More than 150 years ago, Wray and Roy (*1*) observed that ions adsorbed to clays could be exchanged stoichiometrically with ions in solution. On the basis of this observation, a quantitative treatment of retention in ion-exchange chromatography (IEC) has been developed (*2*). In this treatment it is assumed that weakly adsorbed ions (D_b) are displaced from ion exchanging ligands on a chromatographic sorbent by charged groups on a protein (P_o).

$$P_o + Z \cdot D_b \rightleftarrows P_b + Z \cdot D_o$$

The subscripts o and b refer to the free and bound forms of ions, respectively, and Z designates the stoichiometry of the process. In the case of polyelectrolytes, chromatographic retention (k') is related to the number of charges (Z) that interact with a sorbent matrix and the concentration of the displacing agent ($[D_o]$) by the equation $k' = I/[D_o]^Z$. The constant I is composed of a cluster of

---

The author is in the Department of Biochemistry, Purdue University, West Lafayette, IN 47907.